Dimensionality Reduction of Calcium-Imaged Neuronal Population Activity

BMED 7610 – Quantitative Neuroscience – Final Project Report

Group 8:

Chang Woo Choi

Anand Iyer

Yanlin Yang

Abstract

Calcium imaging has gained attention in the neuroscience field for its ability to record large numbers of neurons and thus offer insight into complex neural mechanisms. However, to address the new challenges associated with calcium imaging recordings, we employed a three-step workflow to compare two approaches. First, we created a ground truth for basis of comparison, produced simulated calcium imaging observations from the artificial ground truth, and then modeled the calcium imaging observations into a set of latent variables. In the modeling step, two models were used – one which carried out deconvolution first to remove temporal correlation issues with calcium decay followed by the use of a linear dynamical system (LDS) for dimensionality reduction (Deconv-LDS), and one which carried out both steps simultaneously using a generative model known as a calcium imaging linear dynamical system (CILDS). The results of each model were compared to the ground truth, and it was found that CILDS outperformed across all conditions at the cost of higher computational requirements.

Introduction

The neural models of quantitative neuroscience, such as those discussed in textbooks and during the BMED 7610 course, often capture the mechanisms of only a single or a very small number of neurons. However, complex processes, such as decision-making, motor control and sensorimotor timing, learning, working memory, attention, olfaction, and speech, have

all been demonstrated to have a basis on the behavior of coordinated neuron activity at the population level. Because data at the population level is complex and the subsequent modeling is equally complex, there is a need to apply dimensionality reduction methods to be able to analyze and interpret the data and draw meaningful conclusions applicable to the real world. While dimensionality reduction methods have been used before with traditional electrophysiological recordings, their use and efficacy with other, potentially more complex, sources of neural data have not been well studied. In this project, we will focus on calcium imaging recordings in particular and investigate neural models that incorporate an established dimensionality reduction method and a necessary adjustment. We then try to ascertain whether the models do accurately describe the complex data.

Background

Calcium imaging recordings are an emerging, promising method of data collection in neuroscience thanks to several advantages over traditional electrophysiological methods. Previously, membrane potentials and currents were measured with electrodes or patch-clamps, whereas calcium imaging measures changes in intracellular Ca^{2+} levels with fluorescent indicators that bind to Ca^{2+} ions. The key advantages calcium imaging offers include the ability to record large numbers of neurons, maintain high spatial resolution in the data, and collect data using non-invasive procedures. As noted before, calcium imaging can create datasets of 1-2 orders of magnitude larger than electrophysiology. Nevertheless, calcium imaging does suffer from certain drawbacks, including slow temporal resolution because of the nature of calcium ion decay and uncertainty derived from being an indirect method of data collection with noise artifacts and an unknown ground truth.

To address the above issues, the models in this project will utilize two methods. First, to address the issue of temporal correlation caused by calcium ion decay, which then serve as inputs to the system and create further noise, a deconvolution method will be used to transform calcium imaging observations into spike trains. These spike trains will be used to infer the true activity of the neurons. Second, to reduce high dimensional calcium imaging data into lower dimensions, a linear dynamical system (LDS) will be used to model the neuronal behavior as a small number of latent variables that evolve over time. LDS has been used before in electrophysiological data, particularly time series data studying neural basis of behavior, and has been shown to be quite effective. Thus, we will assess if LDS is appropriate for calcium imaging as well.

Results

To test the models we want to use, we generated a pipeline including 3 steps. First, we generated 10 latent variables by using the Gaussian process as our ground truth. These latent variables were used to create several simulated calcium recording signals, and used two different models to reconstruct latent variables. Finally, we compared the latent variables after reconstruction with ground truth, and quantitatively evaluated the performance of the two models.

1. **Generate the ground truth:** We considered the trial period and temporal resolution in real neural experiments to make the simulated data more realistic. Neural activities related to stimuli responses, for example, are fast. Perceiving visual information only takes 20-50 ms and a typical trial lasts for 1-5 s. Thus, we planned to generate several series of trials that last for 5s and 10 trials in a row.
   First, we employed the Gaussian process (GP) to generate latent variables' baseline. GP is a stochastic process which is used to generate multiple variables following multivariate normal distribution $N(0, K_i)$, where $K_i(t_1, t_2) = \sigma_{f,i}^2 \exp\left(-\frac{(t_1-t_2)^2}{2\tau_i^2}\right) + \sigma_{n,i}^2 \delta_{t_1,t_2}$; $t_1, t_2 \in (0 - T)$; and σ_f and σ_n are the variances of signal and noise, respectively, with a time scale T of 200 ms. Therefore, 10 latent variables were generated by GP as our ground truth, as shown in Fig. 1.

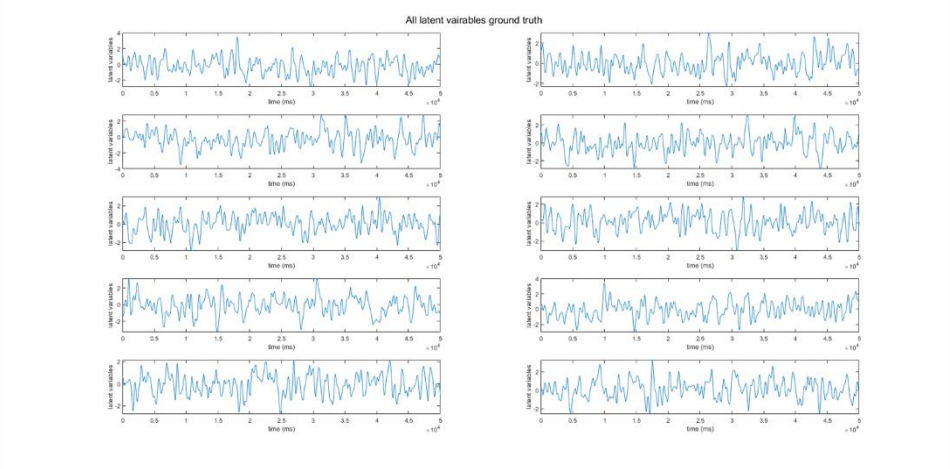

Figure 1. Ground truth latent variables

2. **Generate the simulated data:** After coming up with the ground truth, we projected those 10 latent variables into higher dimensional spaces as a firing rate. The converting expression is $y(t) = ln\left(1 + e^{Az(t)+b}\right)$, where $y(t)$ is the firing rate, $z(t)$ is the vector of latent variables, and $A \in R^{p*q}$ is a loading matrix, such that $p > q$, since the firing rate of neurons is multidimensional compared to latent variables. Moreover,

we added an offset matrix b to add noise. Fig. 2 shows 10 example firing rates out of the whole series of randomly generated firing rates.

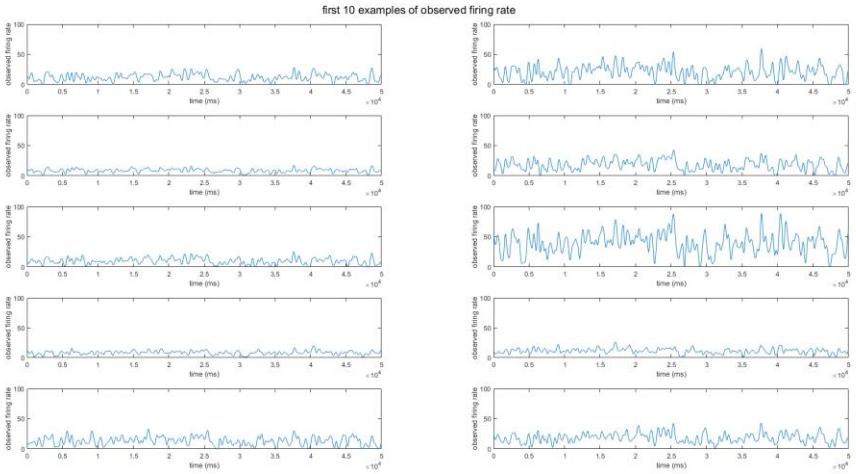

Figure 2. Representative examples of observed firing rates

Next, we created spike trains with generated firing rates. Spike trains at each time point follow the Poisson distribution. Fig. 3 shows an example of 50 spike trains generated by the given firing rate.

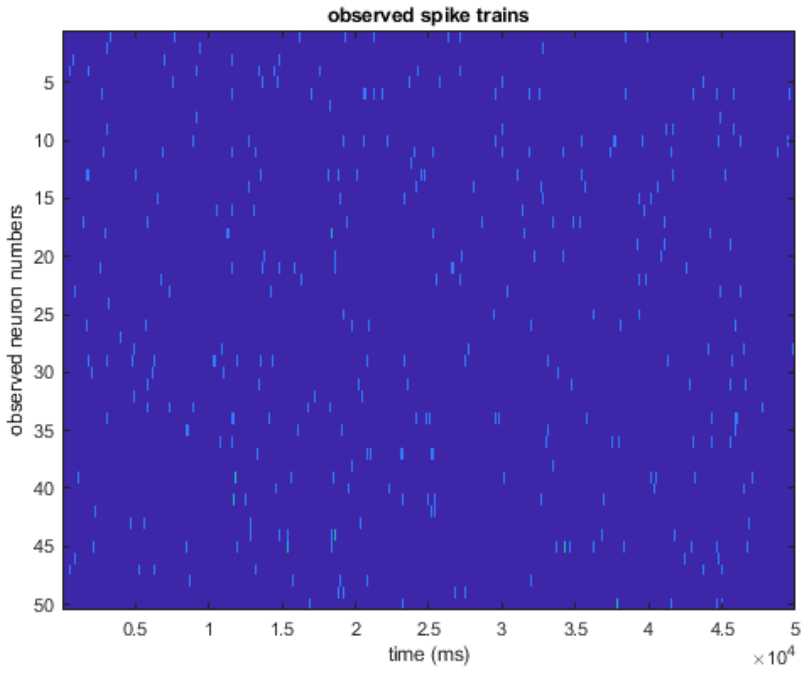

Figure 3. Spike trains from given firing rate

Finally, we generated simulated calcium signal observations from spike trains by convolving calcium decay with the spike trains and adding Gaussian noise to make

them more realistic. Fig. 4 compares calcium signal observations to the previously generated firing rates. As shown, higher firing rates have higher calcium signals, while calcium signals are flat when firing rate is low.

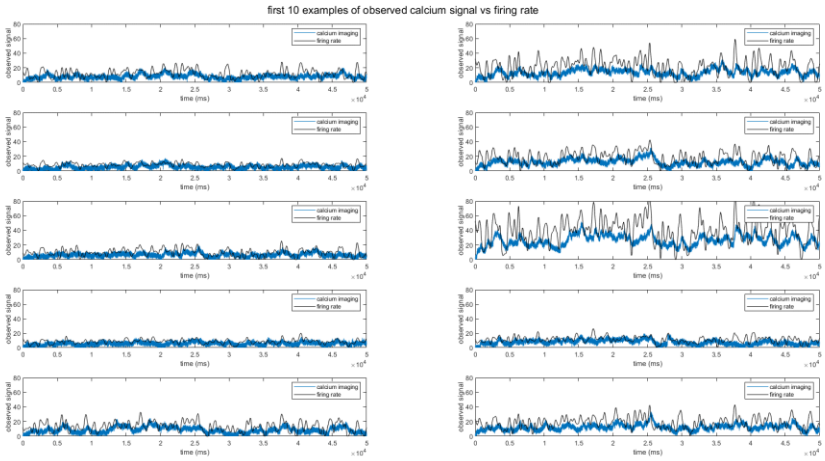

Figure 4. Calcium signals vs. firing rate

3. **Test the two models:** Having generated the calcium signals, we will test the two models in question. Testing the first model (Deconv-LDS) involves executing the two steps of deconvolution and linear dynamical system (LDS) sequentially. In the first deconvolution step, each neuron is deconvolved individually because calcium decay is believed to be independent across different neurons. The model used for this first step is the Online Active Set method to Infer Spikes (OASIS), since it has been shown in literature to be effective at interpreting calcium imaging data. Eq. 1 and 2 is a short mathematical summary of the OASIS model:

$$y_t = ac_t + b + \epsilon_t\,, \qquad \epsilon_t \sim \mathcal{N}(0, \sigma^2) \tag{1}$$

$$c_t = \gamma c_{t-1} + s_t \tag{2}$$

where a is a parameter relating calcium concentration to the measured fluorescence, b represents the base fluorescence, c_t is the calcium concentration, γ is the calcium decay depending on the indicator used, and s_t represents the spiking activity. After each neuron has been deconvolved, we apply a dimensionality reduction procedure using LDS, which can be modeled with the Eq. 3-5.

$$y_t = A\boldsymbol{z}_t + \boldsymbol{b} + \boldsymbol{\epsilon}_t\,, \qquad \boldsymbol{w}_t \sim \mathcal{N}(0, R) \tag{3}$$

$$\boldsymbol{z}_t = D\boldsymbol{z}_{t-1} + \boldsymbol{v}_t\,, \qquad \boldsymbol{v}_t \sim \mathcal{N}(0, P) \tag{4}$$

$$\boldsymbol{z}_1 \sim \mathcal{N}(\boldsymbol{h}_1\,, G_1) \tag{5}$$

where A is a loading matrix, z_t describes the latent variables that describe the system, and D is a dynamics matrix that determines the timescale of the latent variables. An expectation-maximization (EM) algorithm, an iterative method for maximum likelihood estimates, was used to fit the model parameters. Starting off with a random parameter estimate, we calculate the expected value of the log-likelihood of the latent variables, which is then maximized by updating the parameters. This was iterated 500 times to arrive at the final parameters. The results of this first model, the spike trains generated from the deconvolution step and the subsequent latent variables derived in the second step, are shown in Fig. 5 and 6.

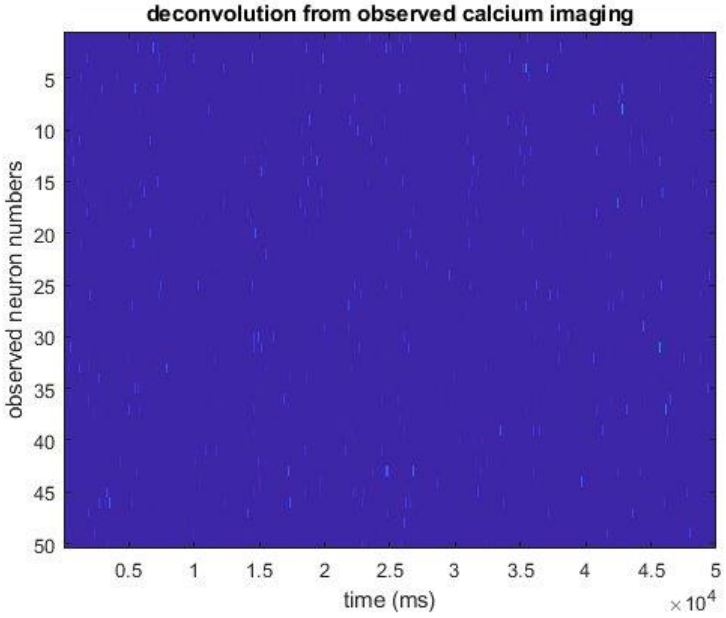

Figure 5. Spike trains from deconvolution

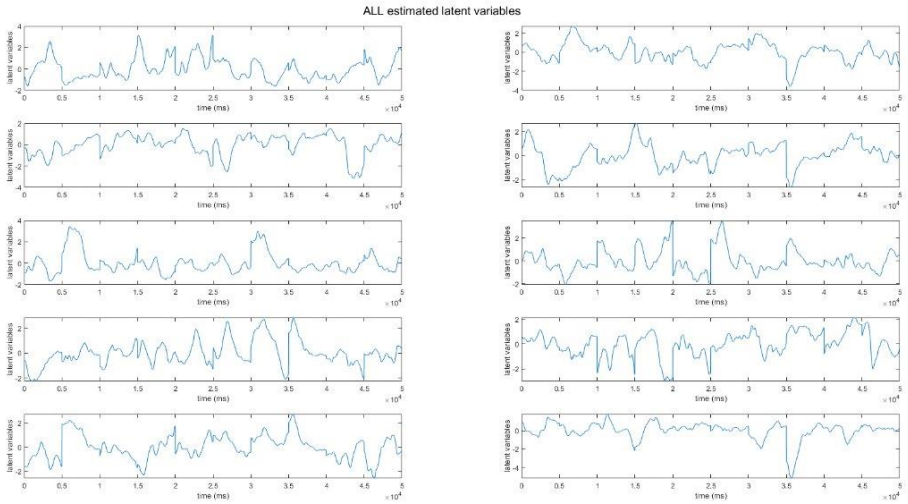

Figure 6. Estimated latent variables from Deconv-LDS

The second model we tested (CILDS) executes both the deconvolution and the LDS modeling concurrently. In other words, all parameters are jointly estimated, rather than individually. The scientific reasoning behind this approach is that because we believe neuronal activity occurs on the scale of groups, not individual neurons, we want to preserve as much shared activity across neurons. By deconvolving each neuron individually in the first model, we are potentially losing some of this shared activity. This combined model, called Calcium Imaging Linear Dynamical System (CILDS) adopted from Koh et. al 2022, can be mathematically summarized with Eq. 6-10.

$$y_t = B\boldsymbol{c}_t + \epsilon_t\,, \qquad \boldsymbol{v}_t \sim \mathcal{N}(0, R) \tag{6}$$

$$\boldsymbol{c}_t = \Gamma\boldsymbol{c}_{t-1} + A\boldsymbol{z}_t + \boldsymbol{b} + \boldsymbol{w}_t\,, \qquad \boldsymbol{w}_t \sim \mathcal{N}(0, Q) \tag{7}$$

$$\boldsymbol{c}_1 \sim \mathcal{N}(\boldsymbol{\mu}_1\,, V_1) \tag{8}$$

$$\boldsymbol{z}_t = D\boldsymbol{z}_{t-1} + \boldsymbol{v}_t\,, \qquad \boldsymbol{v}_t \sim \mathcal{N}(0, P) \tag{9}$$

$$\boldsymbol{z}_2 \sim \mathcal{N}(\boldsymbol{h}_2\,, G_2) \tag{10}$$

where the equations are similar to the first model, with the key innovation of replacing s_t, the spike term, with the LDS term from Eq. 3. All parameters, including B, Γ, A, b, etc., were again jointly estimated using the EM algorithm. The results of this second model (i.e. the reconstruction of the latent variables), are shown in Fig. 7.

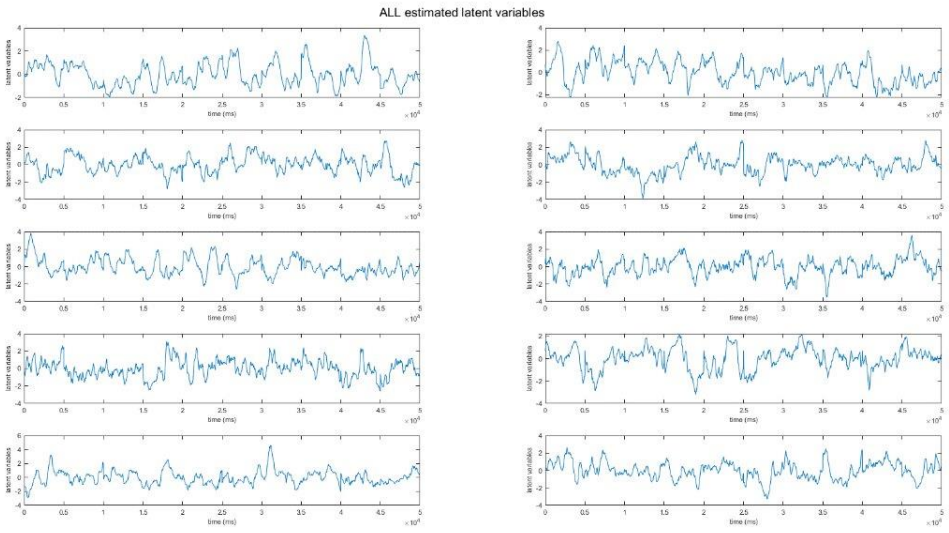

Figure 7. Estimated latent variables from CILDS

4. **Evaluate the models:** As our final step, we compared the estimations of the latent variables from the two models in question and evaluated them against the ground truth variables generated in the first step. Fig. 8 compares the first model (Deconv-LDS) results to the ground truth.

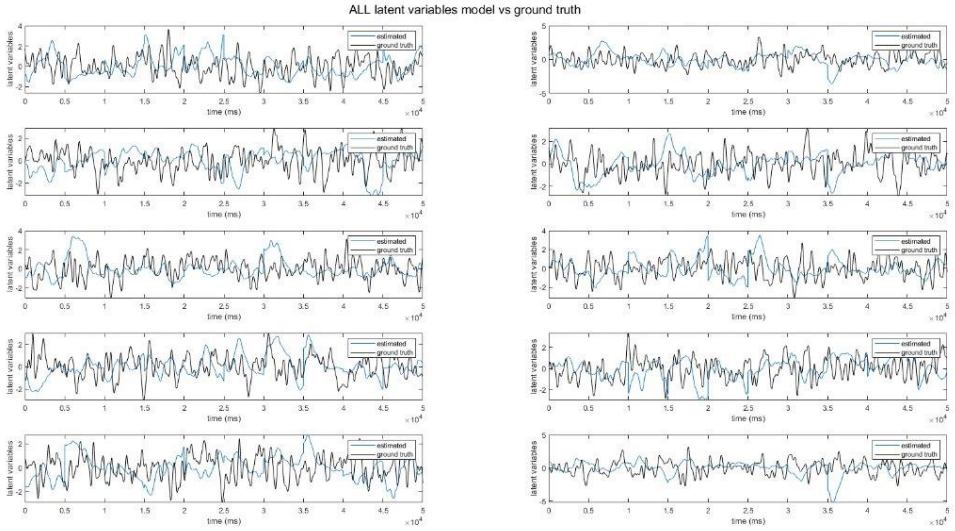

Figure 8. Deconv-LDS vs. ground truth

Comparatively, Fig. 9 evaluates the results of the second model (CILDS) against the ground truth.

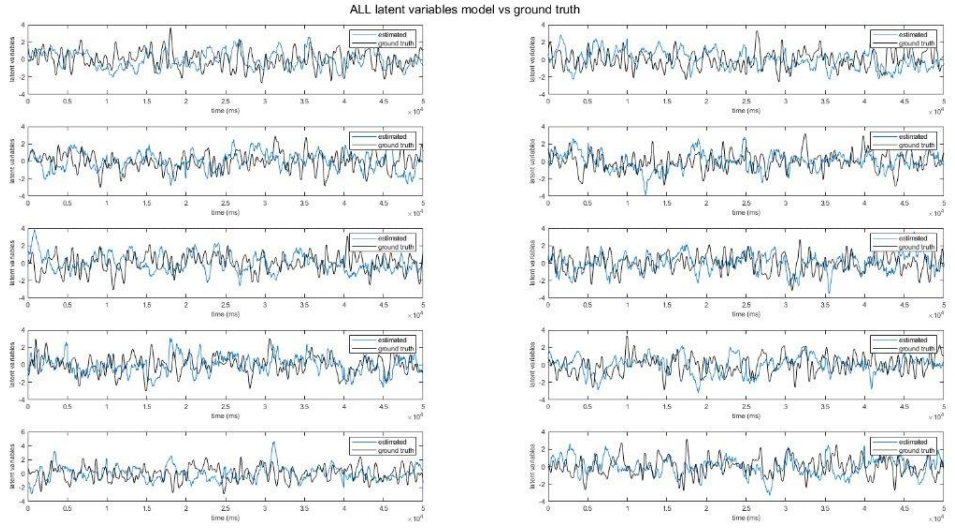

Figure 9. CILDS vs. ground truth

By visual inspection, the second model (CILDS)'s latent variable estimates clearly appear to align more closely with the ground truth values. To formalize this comparison, we calculated a coefficient of determination, defined in Eq. 11.

$$R^2 = 1 - \frac{\sum_{t=1}^{\tilde{T}} \left(z_t^{(i)} - \hat{z}_t^{(i)}\right)^2}{\sum_{t=1}^{\tilde{T}} \left(z_t^{(i)} - \bar{z}^{(i)}\right)^2} \qquad (11)$$

where z_t represents the ground truth latent variables, $\hat{z}_t$ represents the estimated latent variables, and $\bar{z}$ is the mean of the 10 ground truth latent variables. Under one set of common experimental conditions, the R-squared for Deconv-LDS was 0.4235 whereas the R-squared for CILDS was 0.6528. Across all the different conditions tested, CILDS performed with better accuracy.

Discussion

To test how these two models vary under different situations, Koh et. al 2022 already investigated latent variable timescale, neuron numbers, gcamp6 types, and noise. Generally, CILDS performed better than Deconv-LDS. When latent variables' timescale is longer, latent variables become smoother and have low frequency, which means less information for the model and an easier reconstruction. When neuron numbers increase, accuracy also increases as expected since more neurons translate to more information. For gcamp6 types, the less a particular calcium indicator decays, the more accurate the result is. Finally, when the signal is too noisy, it becomes hard to reconstruct the latent variables even if all other parameters are high.

However, Koh et. al 2022 did not consider bin size, which is quite important in neural data analysis. If the bin size is small, the signal is still noisy, and the dataset size remains large. On the other hand, if bin size is large, dataset size decreases significantly, but too much information is lost. Here, we discuss how different bin sizes affect Deconv-LDS and CILDS in two different ways, time consumption and reconstruction accuracy.

As shown in Tables 1 and 2, decreasing bin size increases the computational time, as expected. Interestingly, CILDS spends around 10 times longer time on average for more precise results and the ratio widens as bin sizes get smaller. However, when we consider how bin size correlates with accuracy, the relationship is not linear. 25ms is the best option for bin size among all the values tested. This suggests that there is a local maximum that filters out enough random noise but keeps enough ground truth information. We theorize that this local maximum could be determined by several factors such as the decay rate of the calcium indicator and the unique characteristics of a particular neuron population.

Table 1. Computational time per model by bin size

Bin size (ms)	Deconv-LDS (s)	CILDS (s)
50	2198.205243	15141.645241
25	2579.256160	26432.846632
10	2754.079771	37642.990686
5	2859.037057	48919.307112

Table 2. Accuracy per model by bin size

Bin size (ms)	Deconv-LDS (R-squared)	CILDS (R-squared)
5	0.3888	0.4873
10	0.4472	0.5605
25	0.5437	0.6815
50	0.4624	0.5796

Summary

Complicated mechanisms, such as decision-making, motor control, memory, olfaction, and speech, have been shown to depend on coordinated neuron activity at the population level. Unlike traditional electrophysiological methods which typically record very small numbers of neurons, calcium imaging has emerged as a promising technique to record large numbers of neurons with high spatial resolution. However, to navigate the complexity of calcium imaging data, here we applied deconvolution to address the temporal correlation from calcium decay and LDS to reduce the data into a lower dimension of latent variables. We employed a three-step pipeline in which we generate ground truth variables, generate calcium imaging data from that ground truth, and then estimate latent variables from that data. Two models – Deconv-LDS, a two-step method, and CILDS, a single-step method – were compared using the pipeline. CILDS displayed higher accuracy across all experimental conditions at the cost of consuming more time.

Appendices

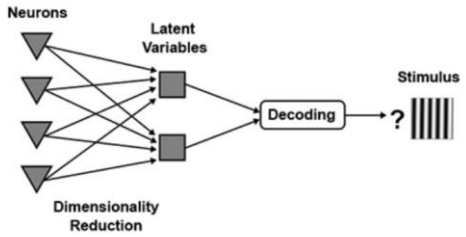

a) Graphic for dimensionality reduction

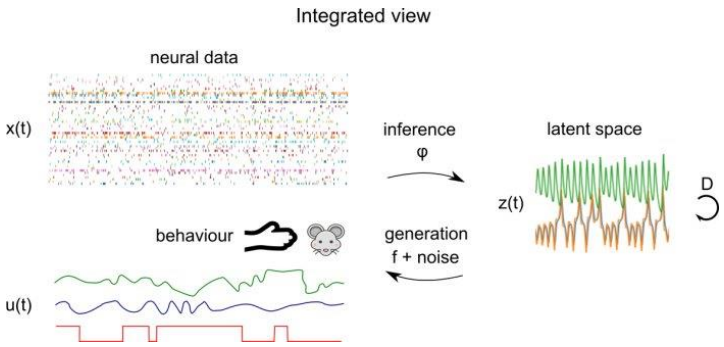

b) Graphic for linear dynamical system

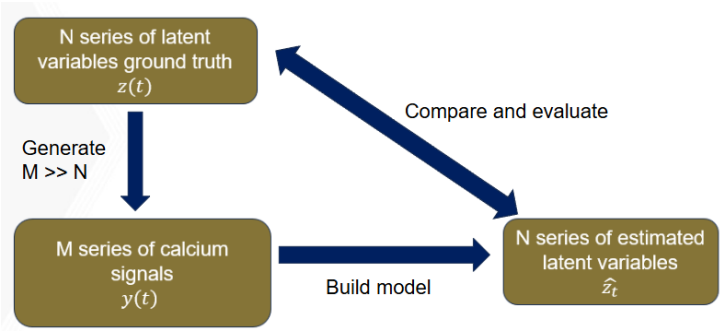

c) Model analysis workflow

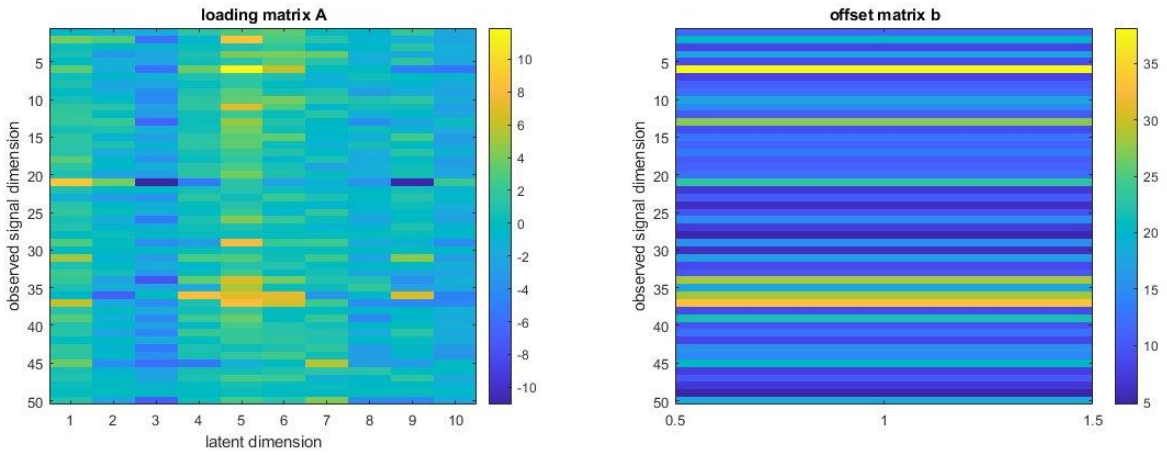

d) Loading and offset matrices dimensions

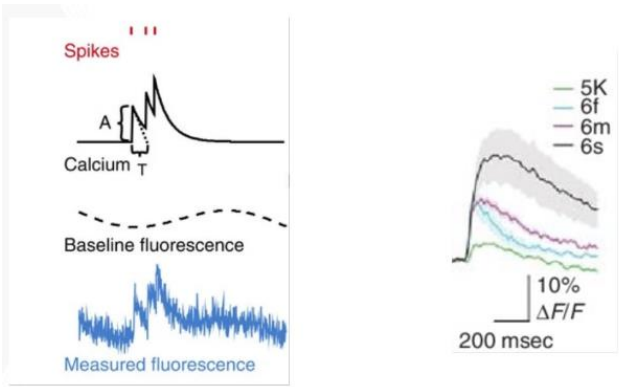

e) Convolution step to generate calcium signals

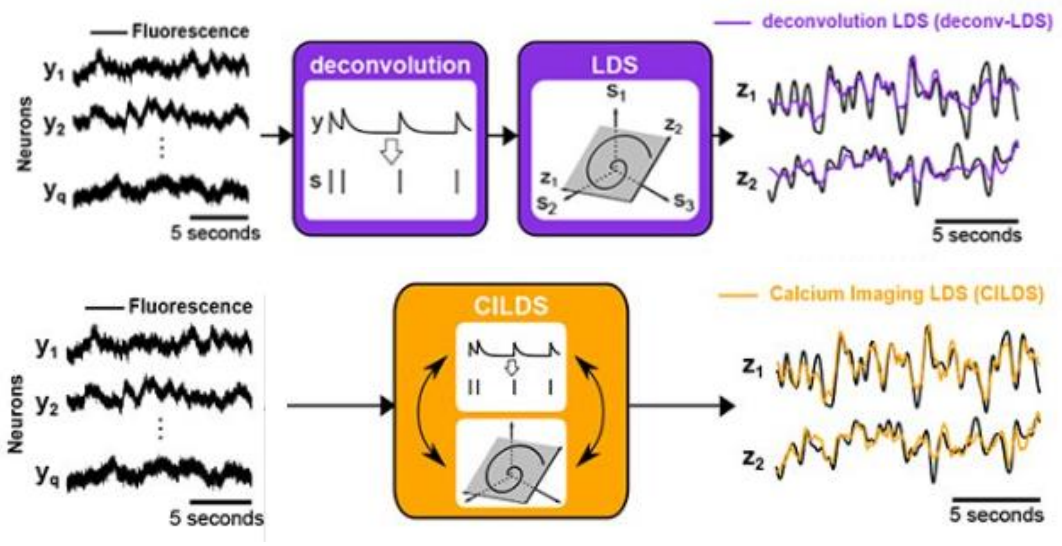

f) Schematic for Deconv-LDS and CILDS

References

- Jercog, Pablo, Thomas Rogerson, and Mark J. Schnitzer. "Large-scale fluorescence calcium-imaging methods for studies of long-term memory in behaving mammals." *Cold Spring Harbor perspectives in biology* 8.5 (2016): a021824.
- Koh, Tze Hui, et al. "Dimensionality reduction of calcium-imaged neuronal population activity." Nature computational science 3.1 (2023): 71-85.
- Sani, Omid G., et al. "Modeling behaviorally relevant neural dynamics enabled by preferential subspace identification." Nature Neuroscience 24.1 (2021): 140-149.
- Deneux, Thomas, et al. "Accurate spike estimation from noisy calcium signals for ultrafast three-dimensional imaging of large neuronal populations in vivo." Nature communications 7.1 (2016): 12190.